

Oceanic Effects on Polar Motion determined from an Ocean Model and Satellite Altimetry: 1993 - 2001

J.L. Chen¹, C.R. Wilson^{1,2}, X.G. Hu³, Y.H. Zhou³, B.D. Tapley¹

¹ Center for Space Research, University of Texas at Austin, Austin, TX 78712, USA

² Department of geological Sciences, University of Texas at Austin, Austin, TX 78712, USA

³ Shanghai Astronomical Observatory, Chinese Academy of Sciences, Shanghai, China

Abstract. Mass redistribution and motion in the oceans are major driving forces of geodetic variations, including polar motion, length-of-day (LOD), geocenter, and gravity field changes. We examine oceanic contribution to polar motion using estimates from a data assimilating ocean general circulation model (OGCM) and satellite radar altimeter observations. The data include OGCM estimates of variations in ocean bottom pressure (OBP) and meridional and zonal velocities. Sea level anomalies from TOPEX/Poseidon (T/P) satellite altimeter measurements and steric sea surface height changes deduced from the model are also used to estimate OBP effects. Estimated oceanic contributions from both OGCM and T/P show considerably better agreement with polar motion observations compared with results from previous studies. The improvement is particularly significant at intra-seasonal time scales. Both OBP and ocean current variations provide important contributions to seasonal polar motion. At intra-seasonal time scales, the oceans appear to be a dominant contributor to residual polar motion not accounted for by the atmosphere. The oceans also play an important role in seasonal excitation. Combined OBP and ocean current contributions explain much of the residual semiannual variability.

Keywords: Polar motion, OGCM, Satellite altimeter, Ocean.

1 Introduction

At time scales of a few years and less, Earth rotational changes (polar motion X and Y, and Length of day (LOD)) are primarily driven by air and water mass redistribution and movement within the Earth system. Atmospheric winds and surface pressure changes are considered to be the dominant contributor to LOD variation [e.g. Barnes et al., 1983; Eubanks et al., 1988a; Hide and Dickey, 1991] and are responsible for a portion of observed polar motion [e.g. Chao and Au, 1991]. Water mass redistribution within the oceans and continental water storage change are also believed to play major roles, particularly for polar motion. Previous studies based on various ocean models [e.g., Dickey et al., 1993; Ponte et al., 1998, 2001; Johnson et al., 1999; Ponte and Ali, 2002; Gross et al., 2003] and satellite radar altimeter measurements [e.g. Chen et al., 2000a] all demonstrate that the

oceans provide important contributions to the excitation of polar motion. However, clear quantitative understanding of oceanic effects on polar motion and LOD remains a challenging goal. A fundamental limitation is the scarcity of observations of the global oceans, which translates into relatively large uncertainties in predictions of ocean general circulation models (OGCM). The two oceanic contributions are from variations in currents and ocean bottom pressure (OBP), and, of these, OBP effects are probably the most difficult to estimate [e.g. Ponte and Stammer, 1999; Hu et al., 2003]. Although satellite altimeters provide nearly global sea surface height (SSH) changes, estimating OBP from them requires removal of steric sea level variations, which are poorly known [e.g., Chen et al., 2000a, b].

Recent advancements in data assimilating OGCMs have inspired new studies of oceanic effects on Earth's rotation and gravity field [Ponte et al., 2001; Dickey et al., 2002; Chen et al., 2003; Gross et al., 2003]. The data-assimilating OGCM [Fukumori et al., 2000], developed at NASA's Jet Propulsion Laboratory (JPL), a partner in the Estimating the Circulation and Climate of the Ocean (ECCO) program provides near real-time estimates of physical changes, including current, SSH, temperature (T), salinity (S), and OBP. The ECCO model calculations are thus a valuable resource in the study of oceanic effects on geodetic observations, and ECCO estimates of T and S provide the information needed to calculate steric SSH changes, caused by seawater density variations.

The T/P satellite radar altimeter and its follow-on Jason-1 have been producing accurate global measurements of SSH every 10 days for over 10 years. T/P SSH changes include two effects, steric changes that do not alter OBP, and mass changes that do. Using T/P SSH data from 1993 to 1996 and a simplified steric SSH model from ocean temperature data taken over many years, Chen et al. (2000a) showed that the oceans may play an important role in driving intra-seasonal polar motion. However, their conclusions were limited, in part by the relatively short duration of T/P data, and, more importantly, by the steric SSH model, which was purely seasonal. A new study of the altimeter data is called for, given the extended period of T/P observations, and the ECCO OGCM which is suitable for estimating time series of steric SSH.

In this study, we investigate oceanic effects on polar motion using ECCO and T/P results, at seasonal and shorter time scales. ECCO estimates of OBP and currents provide one estimate of the entire ocean contribution, while T/P SSH combined with ECCO SSH predictions provide a second OBP estimate. We have not extended the study to LOD because in that case the winds are the dominant excitation source.

2 Theory

Polar motion is excited by mass motion (e.g., winds and currents) and surface mass load (e.g., atmospheric pressure and OBP) variations. The two components of polar motion, χ_1 and χ_2 can be represented as the sum of these two terms,

$$\begin{bmatrix} \chi_1 \\ \chi_2 \end{bmatrix} = \begin{bmatrix} \chi_1^{\text{mass}} \\ \chi_2^{\text{mass}} \end{bmatrix} + \begin{bmatrix} \chi_1^{\text{motion}} \\ \chi_2^{\text{motion}} \end{bmatrix} \quad (1)$$

At a given grid point (latitude ϕ , longitude λ , time t), OBP change represents the integral of mass change of the water column above and can be approximately treated as mass load change, $q(\phi, \lambda, t) = \Delta\text{OBP}/g$ (in units of kg/m^2 ; g gravitational acceleration). Therefore, oceanic excitation of polar motion can be computed as [e.g. Eubanks, 1993],

$$\begin{bmatrix} \chi_1^{\text{mass}} \\ \chi_2^{\text{mass}} \end{bmatrix} = -\frac{1.098 \cdot R_e^2}{(C - A)} \iint q(\phi, \lambda, t) \cdot \sin(\phi) \cos(\phi) \begin{bmatrix} \cos(\lambda) \\ \sin(\lambda) \end{bmatrix} \cdot ds \quad (2)$$

and,

$$\begin{bmatrix} \chi_1^{\text{motion}} \\ \chi_2^{\text{motion}} \end{bmatrix} = \frac{1.5913 R_e}{(C - A) \Omega_0} \iiint \cos(\phi) \cdot \left(U(\phi, \lambda, h, t) \cdot \begin{bmatrix} -\cos(\lambda) \sin(\phi) \\ -\sin(\lambda) \sin(\phi) \end{bmatrix} + V(\phi, \lambda, h, t) \cdot \begin{bmatrix} \sin(\lambda) \\ -\cos(\lambda) \end{bmatrix} \right) \cdot dm \quad (3)$$

in which, R_e and Ω_0 are the Earth's mean radius and angular velocity, A and C the Earth's principal moments of inertia, and U and V the zonal and meridional velocities of currents. $ds = R_e^2 \cos(\phi) d\phi d\lambda$ is the surface area element and $dm = \rho \cdot R_e^2 \cos(\phi) d\phi d\lambda dh$, is the mass element of a given grid box. ρ is the density of seawater, h the layer depth, and dh the layer thickness. Since density only changes slightly with

temperature, salinity, and pressure change (typically below the 1% level), we use a constant mean density ($\rho_0=1.028 \text{ g/cm}^3$) in computing ocean current excitations.

3. Data and Models

3.1 The ECCO/JPL Model

The ECCO OGCM is based on the parallel version of the Massachusetts Institute of Technology general circulation model and an approximate Kalman filter method [Fukumori et al., 2000]. The ECCO model (run kf047a) assimilates T/P SSH observations. The model coverage is nearly global from $-79^\circ.5\text{S}$ to $78^\circ.5\text{N}$ and has a telescoping meridional grid with a 1/3-degree resolution in the tropics (-20°S to 20°N) that gradually increases to a 1-degree resolution away from the equator. The resolution in longitude is 1 degree. There are 46 vertical levels with 10m resolution within 150m of the surface. The model is forced by NCEP reanalysis products [Kalnay et al., 1996] (12-hourly wind stress, daily heat and fresh water fluxes) with time-means replaced by those of the Comprehensive Ocean-Atmosphere Data Set. Temperature and salinity at the model sea surface are relaxed towards observed values. Model fields are available at 10-day intervals (as 10-day averages). SSH and OBP are also available at 12-hour intervals (as instantaneous values).

The ECCO values used here include 10-day averaged OBP, SSH, zonal (U) and meridional (V) velocities, from January 1993 to December 2001. We use ECCO T and S changes to estimate steric SSH change, to provide a correction for T/P SSH. The ECCO model employs the Bossiness approximation to conserve total ocean volume. This will cause changes of estimated total ocean mass unrelated to any oceanographic effect. To correct this, we enforce ECCO mass conservation by removing a mean OBP (over the oceans) at each time step [Greatbatch, 1994]. This correction is not required for T/P-derived OBP change because T/P measures real sea level change, including effects of water exchange between the oceans and other elements of the Earth system [e.g. Chen et al., 1998; Minster et al., 1999].

3.2 T/P SSH Observations and ECCO Steric Estimates

T/P SSH data are from the JPL World Ocean Circulation Experiment (WOCE) Satellite Data DVD-ROM (Version 3.0, <http://podaac.jpl.nasa.gov/woce>). The data are given on a $1^\circ \times 1^\circ$ grid (via Gossip interpolation) every 5 days from October 1992 to December 2001. The portion overlapping the ECCO results (January, 1993 to December, 2001) is used here. We resampled the T/P data to the ECCO 10-day interval. Atmospheric inverted barometer (IB) effects on sea level change have been corrected using NCEP reanalysis surface pressure data (see details at http://podaac.jpl.nasa.gov/woce/woce3_topex/topex/docs/topex_doc.htm).

OBP variations are the difference between SSH and steric SSH change [e.g., Chen et al., 2000b], so $\Delta OBP = g \cdot \rho_0 \cdot (SSH - SSH_{steric})$, where

$$SSH_{steric} = -\frac{1}{\rho_0} \cdot \int_{-h}^0 \Delta \rho \cdot dh \quad (4)$$

and where $\Delta \rho$ is the density change as a function of T, S, and pressure (P). The integral is from the ocean bottom to the surface ($h=0$). $\Delta \rho$ is computed using the United Nations Educational, Scientific and Cultural Organization (UNESCO) 1983 algorithm [Fofonoff and Millard, 1983]. Using Equation 4, we compute SSH_{steric} using T, S, and P (P is inferred from layer depths) from the ECCO model, and then combine them with T/P data.

3.3 Polar Motion Observations and Atmospheric Effects

Polar motion X and Y time series are from SPACE2001 [Gross, 2002], obtained from various space geodetic observations (VLBI, GPS, SLR, and LLR) through a Kalman filter combination [Eubanks, 1988]. The data cover the period September 1976 through January 2002, with daily sampling. X and Y time series are averaged and resampled at the same 10-day interval as ECCO results. Sub-daily tidal corrections have been removed from X and Y series [Gross, 2002]. Polar motion excitations χ_1 and χ_2 are derived from X and Y using the discrete polar motion equation of Wilson (1985).

Atmospheric wind and surface pressure effects on χ_1 and χ_2 are removed using NCEP reanalysis

atmospheric angular momentum (AAM) results provided by Atmospheric and Environmental Research [Salstein and Rosen, 1997]. IB effects are corrected in the same way as for T/P SSH data. Wind excitations are computed by integrating the horizontal winds from the surface to the top of the model at 10 hPa. The daily excitations from SPACE 2001 and 6-hourly AAM time series are averaged and resampled at the same 10-day intervals as the ECCO model. Residuals after subtracting atmospheric effects, are expected to be dominantly due to the oceans and continental water storage changes.

4. Results and Comparison

4.1 Contributions from OBP Change

Oceanic contributions to X and Y from ECCO OBP are shown in Figures 1a and 1b (blue curves). The residual variations of X and Y (i.e., SPACE2001 minus atmospheric effects) are in gray. Figures 1a and 1b also show (in green curves) contributions from T/P derived OBP change. Clearly, oceanic mass redistribution (OBP changes) is responsible for a significant portion of residual X and Y variations over a broad band of frequencies. Both ECCO and T/P predictions agree reasonably well with the residuals.

To have a closer look at seasonal frequencies, we estimate amplitudes and phases of annual and semiannual variations from time series in Figure 1 by least squares, with results in Table 1. OBP change is an important source of seasonal polar motion. T/P OBP predicts relatively larger annual and semiannual changes in X, compared with ECCO, but smaller changes in Y. The phases of the semi-annual terms agree very well (see Table 1), although agreement of annual phases is relatively poor. We removed annual and semiannual sinusoidal terms from all time series and show the remaining intra-seasonal variations in Figure 2a and 2b. Agreement between polar motion observations and OBP predictions is evident.

4.2 Contributions from Ocean Current

Contributions from ECCO ocean currents (U&V) are shown in red in Figures 1a and 1b, with non-seasonal excitations in red in Figure 2a and 2b. Ocean current effects also agree well with residual X and Y variations over a broad band of frequencies and appear

as important as OBP in driving polar motion. Figure 3a and 3b show combined oceanic effects ECCO OBP + U&V (green) and T/P OBP + ECCO U&V (red) compared with the residual X and Y (blue). Total ocean contributions, either ECCO OBP + U&V or T/P OBP + ECCO U&V agree better with residual X and Y than either separately.

Annual and semiannual amplitudes and phases of the combined series are obtained by least squares, with results in Table 1. ECCO seasonal ocean current effects on X are greater than OBP, and are similar in the Y component. Discrepancies at seasonal frequencies in Table 1 are expected because continental water storage change, not considered here, is likely to have an important effect on seasonal polar motion [e.g. Chao and O'Connor, 1988; Kuehne and Wilson, 1991; Chen et al., 2000a]. Thus Table 1 mainly illustrates the relative size of individual and combined oceanic effects (OBP, current, and OBP + Current) on X and Y. To close the budget, effects from all sources (atmosphere, ocean, and continental water) need to be estimated in a fully consistent way.

Figure 4a and 4b compare intra-seasonal X and Y residuals and two combined oceanic excitations (i.e., ECCO OBP + U&V, and T/P OBP+ECCO U&V). Combined OBP and ocean current effects improve the agreement with X and Y residuals. Thus, oceanic mass redistribution and currents are major contributors to these non-atmospheric X,Y residuals.

4.3 Cross Correlation and Variance Analysis

We compute normalized cross correlations between intra-seasonal time series in Figure 2a, 2b, 4a, and 4b, with Table 2 giving the zero-lag correlation coefficients. Percentage variance reductions associated with subtracting each oceanic contribution from observed X,Y residuals are also listed in Table 2. As an example, Figure 5a and 5b show the cross correlation between (X, Y) and estimates from ECCO-OBP and T/P- OBP. Figures 5a and 5b and Table 2 show clearly that estimated OBP and current excitations are strongly correlated with non-atmospheric residual X and Y excitations. ECCO (OBP + current) excitations show stronger correlations in X (0.76 vs. 0.68) and explain a relatively larger portion of the variance (57% vs. 46%). However, for Y, T/P OBP (+ECCO currents) provides better

agreement (0.81 vs. 0.79), and explains more of the variance than the full ECCO estimate (63% vs. 60%). Combined excitations, both ECCO OBP + U&V and T/P OBP + ECCO U&V can explain more variance than either OBP or currents, separately

We also list in Table 1 very recent estimates of annual and semiannual amplitude and phase from the OAM time series published by Gross et al., [2003]. These are from an ECCO OGCM run that was not data-assimilating. These results are averaged and resampled at the same 10-day intervals, and determined from exactly the same time period 1993-2001. Cross correlation and variance reduction at intra-seasonal time scales are also listed in Table 2 for these series. This non-data-assimilating ECCO run predicts relatively smaller annual excitation in X and slightly larger in Y compared with the data assimilating ECCO calculation used in our study. Semiannual excitations estimated from the data assimilating ECCO model (used in this study) and T/P OBP (+ECCO currents) agree apparently better with observations than those from the non-data-assimilating ECCO run. For the non-seasonal residuals, estimates from the data assimilating ECCO and T/P OBP (+ECCO currents) also agree significantly better (with observations) in term of both correlation and variance reduction, especially in the Y component (see Table 2).

4.4 Power and Coherence Spectrum Analysis

We compute power spectrum densities of non-atmospheric residuals in X and Y and compare them with spectra of the two combined estimates of oceanic contributions, shown in Figures 6a and 6b. At seasonal or shorter time scales, oceanic contributions agree well with SP01-AAM residuals in X and Y. The annual variation appears dominant in both X and Y, while the semiannual variation is also significant in X. This is consistent to the values in Table 1.

Figures 7a to 7d show magnitudes and phases of the coherence between non-atmospheric residuals and two oceanic excitations, ECCO OBP + U&V and T/P OBP + ECCO U&V. Mean and trend are removed from all time series. Annual and semiannual variations have also been removed by least squares fitting. The two dashed lines in Figure 7a and 7b represent the 95% and 99% confidence level. Both ECCO and T/P based excitations show good correlation with SP01-AAM residuals over much of the intra-seasonal frequency

band. The ECCO estimates show better coherence with the SPACE-AAM residuals in X, while T/P (+ ECCO U&V) appears showing better agreement in Y. This is consistent with the results from cross correlation and variance reduction analysis (see Table 2).

5. Discussion

Predictions from the data assimilating ECCO model and T/P altimeter measurements show the oceans to be a major contributor to observed polar motion, especially at seasonal and intra-seasonal time scales. Oceanic mass (OBP) and current changes are comparably important in affecting polar motion. The combined oceanic effects (based on either ECCO or T/P + ECCO) appear to be a major contributor to the remaining intra-seasonal variations in X and Y. At annual period, ECCO and T/P + ECCO can more than explain non-atmospheric X residuals and provide comparable estimates for Y. At the semiannual period, the two estimates explain a majority part of the residual signals, especially in X (see Figure 8 and Table 1).

Compared with previous studies, we find improved agreement between estimates of ocean contributions and observed polar motion. The data assimilating ECCO model estimates thus appear superior to POCM in modeling large scale oceanic mass and current changes. The improvement in correlation coefficients is significant (e.g. 0.76/0.79 from this study v.s. 0.38 from that of Johnson et al. [1999], based on the POCM model). Our findings are in general agreement with those of Gross et al. [2003], based on the ECCO non-data-assimilating model. However we find that the data assimilating ECCO model used here leads to better agreement with observed polar motion (see Table 1). This is also true for the non-seasonal residuals (see Table 2).

The T/P based predictions (T/P OBP + ECCO U&V) show significant improvement in agreement with X and Y residuals when compared with previous results [e.g. Chen et al., 2000a]. This is attributed to availability of a longer T/P data set, and the employment of ECCO to estimate steric SSH. Steric effects account for a majority part of observed sea level change [e.g. Chen et al., 2000b], and are a critical element in using altimeter data to infer oceanic mass redistribution. The apparent success in estimating

steric effects from ECCO demonstrates that altimeter observations can be a valuable data resource in studies of oceanic mass variations and redistribution.

Agreement between OGCM predictions and observed polar motion is remarkably good, considering the possibilities for inadequacies in OGCM results. OBP current estimates, especially at depth, are virtually unconstrained by observations, so it is difficult to assess errors. The same goes for T and S, especially at depth. In the case of OBP, the difference between two temporally correlated quantities (SSH and SSH_{steric}) of about the same size, there is a good chance that errors will contaminate the estimates. The Bossiness approximation (conserving ocean volume) forces an ad-hoc adjustment (the Greatbatch convention) to conserve mass. Non-global coverage of both the OGCM and T/P may be a problem as well. A mass-conserving OGCM [e.g., Huang et al., 2001] that assimilates altimeter sea level, sea surface temperature, and salinity data and is driven by winds, fluxes, and also atmospheric pressure is clearly the next step. In the longer term, fully coupled models that conserve mass within the full atmosphere-ocean-hydrosphere system are needed. Assimilation of satellite gravity observations, such as from the Gravity Recovery and Climate Experiment mission would likely be an important improvement in OGCM development, as well.

Acknowledgments. We thank Richard Gross, Thomas Johnson, and another anonymous reviewer for their insightful comments, which led to improvements in the presentation. We are grateful to the ECCO team for providing the model data, with special thanks to Zhangfan Xing and Benyang Tang for help in extracting and interpreting the data. We would like to thank Atmospheric and Environmental Research, and their activities organized under the International Earth Rotation Service for providing the NCEP reanalysis AAM data. This research was supported by NASA's Solid Earth and Natural Hazards Program.

References:

Barnes, R., R. Hide, A. White, and C. Wilson, Atmospheric angular momentum functions, length-of-day changes and polar motion, Proc. R. Soc. Lond., A387, 31-73, 1983.

- Chao, B., F. and W. P. O'Connor, Effect of a uniform sea-level change on the Earth's rotation and gravitational field, *Geophys. J., R. astr. Soc.*, 93, 191-193, 1988.
- Chao, B. F., and A. Y. Au, Atmospheric Excitation of the Earth's Annual Wobble: 1980-1988, *J. Geophys. Res.*, 96, 6577-6582, 1991.
- Chen, J.L., C.R. Wilson, D.P. Chambers, R.S. Nerem, and B.D. Tapley, Seasonal Global Water Mass Budget and Mean Sea Level Variations, *Geophys. Res. Lett.*, 25 (19), 3555-3558, 1998.
- Chen, J.L., C.R. Wilson, B.F. Chao, C.K. Shum, and B.D. Tapley, Hydrologic and Oceanic Excitations to Polar Motion and Length-of-day Variation, *G. J. Internat.*, Vol. 141, 149-156, 2000a.
- Chen, J.L., C.K. Shum, C.R. Wilson, and D.P. Chambers, B.D. Tapley, Seasonal Sea Level Change from TOPEX/Poseidon Observation and Thermal Contribution, *Journal of Geodesy*, 73, 638-647, 2000b.
- Chen, J.L., C.R. Wilson, X.G. Hu, B.D. Tapley, Large-Scale Mass Redistribution in the Oceans, 1993 - 2001, *Geophys. Res. Lett.*, Vol. 30, No. 20, 2024, 2003.
- Dickey, J.O., S.L. Marcu.; C.M. Johns, R. Hide, and S.R. Thompson, The oceanic contribution to the Earth's seasonal angular momentum budget, *Geophys. Res. Lett.*, 20 (24), 2953-2956, 1993.
- Dickey, J.O., S.L. Marcus, Olivier de Viron, I. Fukumori, Recent Earth Oblateness Variations: Unraveling Climate and Postglacial Rebound Effects, *Science*, 298, 1975-1977, 2002.
- Eubanks, T.M., J.A. Steppe, J.O. Dickey, R.D. Rosen, and D.A. Salstein, Causes of Rapid Motions of the Earth's Pole, *Nature*, 334, 115 - 119, 1988a.
- Eubanks, T.M., Combined Earth rotation series smoothed by a Kalman filter, in Bureau International de l'Heure Annual Report for 1987, pp. D85-D86, Obs. de Paris, Paris, 1988b.
- Eubanks, T.M., Variations in the orientation of the earth, in Contributions of Space Geodesy to Geodynamic: Earth Dynamics, *Geodyn. Ser.*, vol. 24, edited by D. Smith and D. Turcotte, pp. 1-54, AGU, Washington, D.C., 1993.
- Fofonoff, P. and Millard, R.C. Jr, Unesco 1983. Algorithms for computation of fundamental properties of seawater, 1983. Unesco Tech. Pap. in *Mar. Sci.*, No. 44, 53 pp.
- Fukumori, I., T. Lee, D. Menemenlis, L.-L. Fu, B. Cheng, B. Tang, Z. Xing, and R. Giering, A Dual Assimilation System for Satellite Altimetry, Joint

- TOPEX/POSEIDON and Jason-1 Science
Working Team Meeting, Miami Beach, Florida,
15-17 November 2000.
- Greatbatch RJ, A note on the representation of steric
sea level in models that conserve volume rather
than mass, *J. Geophys. Res.*, 99, 12,767-12,771,
1994.
- Gross, R., Combinations of Earth Orientation
Measurements, SPACE2001, COMB2001, and
POLE2001, Jet Propulsion Laboratory Pub. 02-08,
27 pp., Pasadena, Calif., 2002.
- Gross, R.S., I. Fukumori, and D. Menemenlis,
Atmospheric and Oceanic Excitation of the Earth's
Wobbles During 1980-2000, *J. Geophys. Res.*,
VOL. 108, NO. B8, 2370,
doi:10.1029/2002JB002143, 2003.
- Hide, R. and J.O. Dickey, Earth's variable rotation,
Science, 253, 629 - 637, 1991.
- Hu, X.G., J.L. Chen, B.D. Tapley, C.R. Wilson, Ocean
Bottom Pressure Variability, A Study with Ocean
General Circulation Models, Satellite Altimetry,
and In-Situ Measurements, *J. Geodesy*, 2003 (in
review).
- Huang, R. X., X.-Z. Jin, and X.-H. Zhang, An ocean
general circulation model in pressure coordinates.
Advances in Atmospheric Science, **18**, 1-22, 2001
- Johnson, T.J., C.R. Wilson, and B.F. Chao, Oceanic
angular momentum variability estimated from the
Parallel Ocean Climate Model, 1988-1998, *J.
Geophys. Res.*, 104(B11), 25,183-25,195, 1999.
- Kalnay, E., et al., "The NCEP/NCAR 40-year
reanalysis project," *Bulletin of the American
Meteorological Society*, **77**, 437-471, 1996.
- Kuehne, J., and C. R. Wilson, Terrestrial Water
Storage and Polar Motion, *J. Geophys. Res.*, 96,
4337-4345, 1991.
- Marcus, Steve, Yi Chao, Jean Dickey, and Pascal
Gegout, Detection and Modeling of NonTidal
Oceanic Effects on Earth's Rotation Rate, *Science*,
1656-1659, 1998.
- Minster, J.F., A. Cazenave, Y.V. Serafini, F. Mercier,
M.C. Gennero, P. Rogel, Annual cycle in mean
sea level from TOPEX-Poseidon and ERS-1:
inference on the global hydrological cycle, *Global
and Planetary Change*, **20**, Page 57-66, 1999.
- Ponte, R.M., D. Stammer, and J. Marshall, Oceanic
signals in observed motions of the Earth's pole of
rotation, *Nature*, 391, 476-479, 1998
- Ponte, R.M., and D. Stammer, Role of ocean currents
and bottom pressure variability on seasonal polar

- motion, *J. Geophys. Res.*, 104 (C10), 23,393-23,410, 1999.
- Ponte, R.M., D. Stammer, and C. Wunsch, Improving ocean angular momentum estimates using a model constrained by data, *Geophys. Res. Lett.*, 28 (9), 1775-1778, 2001.
- Ponte, R.M., and A.H. Ali, Rapid ocean signals in polar motion and length of day, *Geophys. Res. Lett.*, 29 (15), 6-1 to 6-4, 2002.
- Salstein, D.A., and R.D. Rosen, Global momentum and energy signals from reanalysis systems. Preprints, 7th Conf. on Climate Variations, American Meteorological Society, Boston, MA, 344-348, 1997.
- Wilson, C.R., Discrete Polar Motion Equations, *Geophys. J. R. astr. Soc.*, 80, 551-554, 1985.

Figures:

Figure 1 a) Oceanic effects on polar motion X from ECCO OBP (blue curve), T/P derived OBP (green curve), and ECCO ocean current (red curve), compared with SPACE2001 -NCEP AAM (gray curve). b) Same as in a), but for polar motion Y.

Figure 2 a) Intra-seasonal oceanic effects on polar motion X from ECCO OBP (blue curve), T/P derived OBP (green curve), and ECCO ocean current (red curve), compared with SPACE2001 -NCEP AAM (gray curve). b) Same as in a), but for polar motion Y.

Figure 3 a) Combined oceanic effects on polar motion X from ECCO OBP + U & V (green curve) and T/P OBP + ECCO U & V (red curve), compared with SPACE2001 -NCEP AAM (blue curve). b) Same as in a), but for polar motion Y.

Figure 4 a) Intra-seasonal combined oceanic effects on polar motion X from ECCO OBP + U & V (green curve) and T/P OBP + ECCO U & V (red curve), compared with SPACE2001 -NCEP AAM (blue curve). b) Same as in a), but for polar motion Y.

Figure 5 a) Cross correlation coefficients between T/P derive OBP effects and residual X (blue curve) and between ECCO OBP effects and residual X (red curve). b) Same as in a), but for polar motion Y.

Figure 6 a) Power spectrum densities of residual X (blue curve), contributions from ECCO OBP + U & V (green curve), and T/P OBP + ECCO U & V (red curve), estimated using the Burg method (with order of 72). b) Same as in a), but for Y.

Figure 7 a) Magnitude and c) phase of the squared coherence (for X) of SPACE2001 -NCEP AAM with oceanic excitations from ECCO OBP + U & V (blue curve) and T/P OBP + ECCO U & V (red curve). b) and d) are show the same analysis and comparison for Y. Annual and semiannual variations have been removed from all time series by least squares fitting. Mean and trend are also removed.

Figure 8 a) Phasor plots for semiannual variations estimated from SPACE2001-AAM residuals and oceanic excitations in X. b) Same as in a), but for Y.

Table 1. Amplitude and phase of annual and semiannual polar motion excitations (X, Y) from observations (SPACE2001-AAM), ECCO, and T/P predictions The phase is defined as ϕ in $\sin(2\pi(t - t_0) + \phi)$, where t_0 refers to h^0 on January 1. Similar estimates from the OAM time series of Gross et al. (2003) are also listed for comparison.

Polar Motion X, Y	X Annual		X Semiannual		Y Annual		Y Semiannual	
	Amplitude (mas)	Phase (deg)						
SPACE2001 - AAM	7.71	52.1	6.14	250.0	13.50	49.6	3.89	174.1
ECCO OBP	2.05	147.8	2.79	238.9	1.50	72.8	2.24	214.6
T/P OBP	5.26	117.0	4.01	252.2	4.57	130.1	0.93	205.0
ECCO U&V	5.01	99.0	2.52	246.6	5.72	79.8	2.25	219.4
ECCO OBP + U&V	6.62	112.5	5.29	242.6	7.21	78.4	4.49	217.0
T/P OBP + ECCO U&V	10.22	108.2	6.52	250.1	5.53	116.9	3.17	211.8
OAM (Gross et al., 2003)	4.75	100.7	5.03	240.1	8.43	71.3	2.22	231.5

Table 2 Cross correlation coefficients between intra-seasonal polar motion (X, Y) not accounted for by the atmosphere (i.e. SPACE2001 - AAM) and effects from the oceans, and variance reduction (in percentage) when the oceanic excitations are removed from SPACE2001 - AAM.

Excitation Source	PM X: SPACE2001 - AAM		PM Y: SPACE2001 - AAM	
	Max. Correlation	Reduced Variance	Max. Correlation	Reduced Variance
ECCO OBP	0.65	40%	0.72	46%
T/P OBP	0.56	31%	0.76	49%
ECCO U&V	0.52	25%	0.72	29%
ECCO OBP + U&V	0.76	57%	0.79	60%
T/P OBP + ECCO U&V	0.68	46%	0.81	63%
OAM (Gross et al., 2003)	0.73	52%	0.63	40%

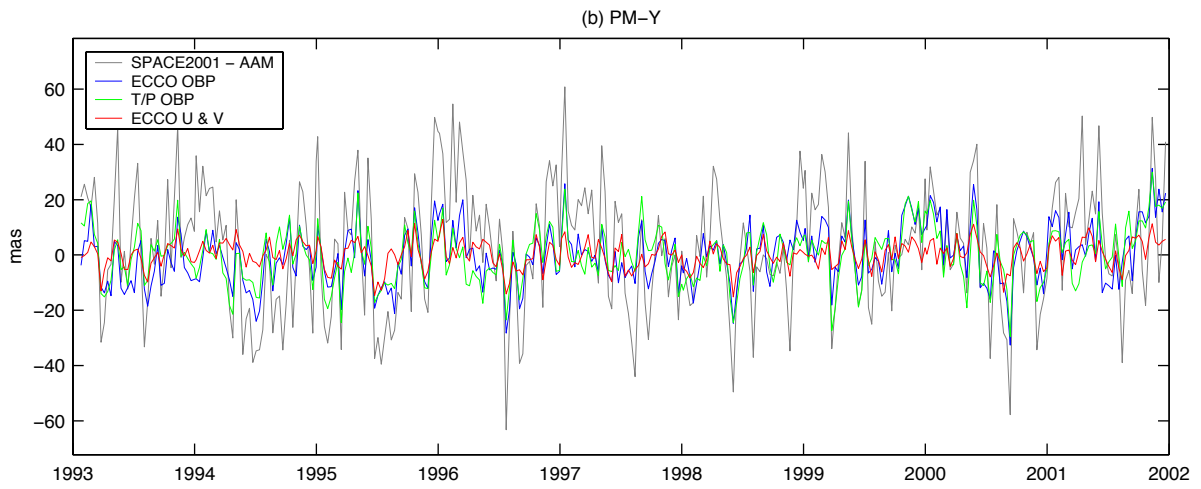
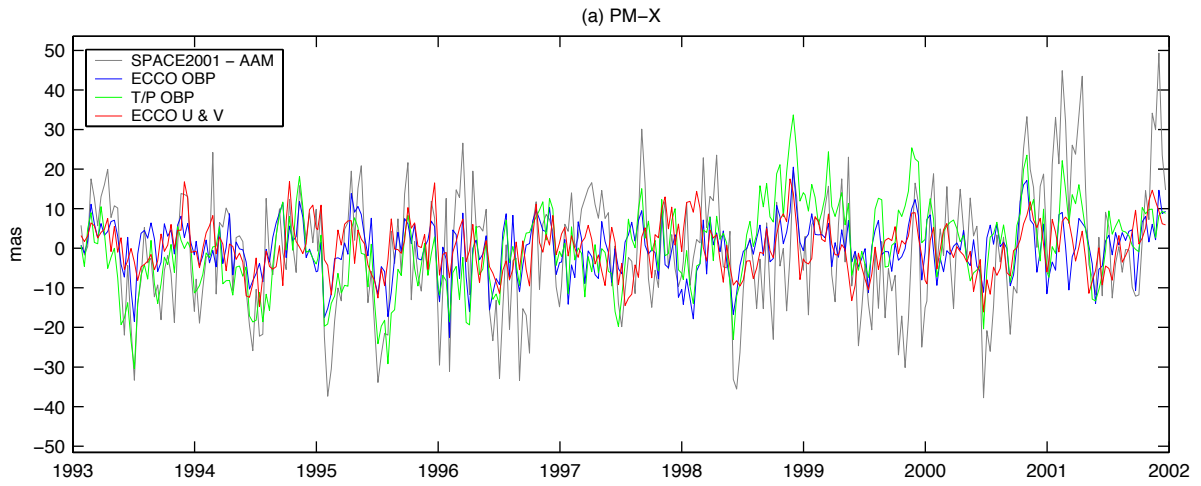


Figure 1

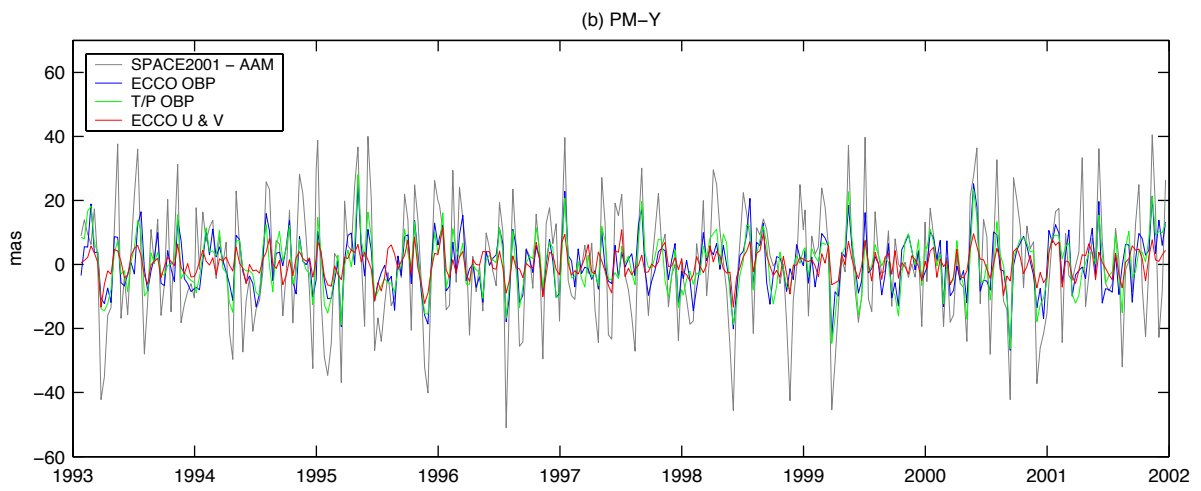
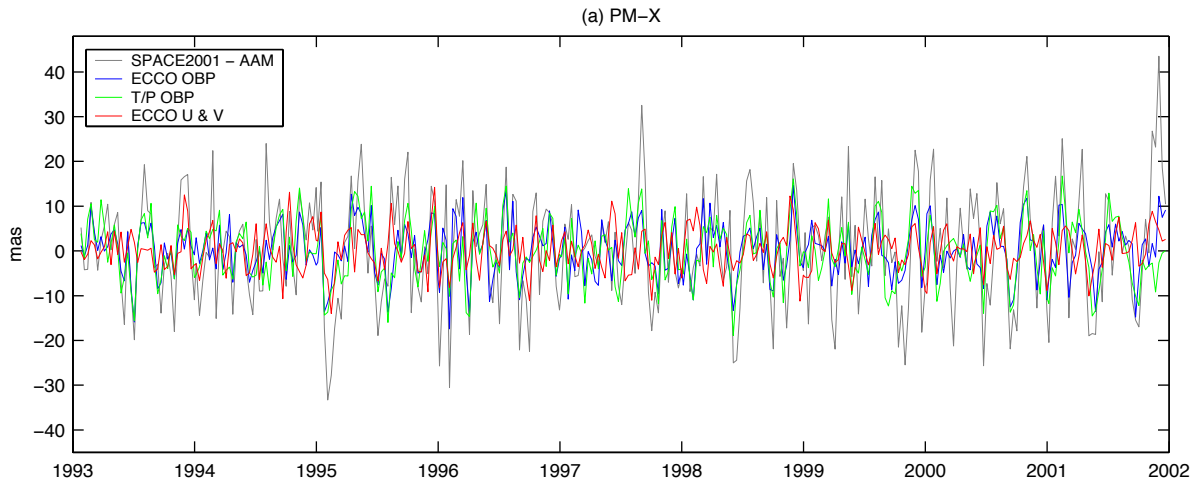


Figure 2

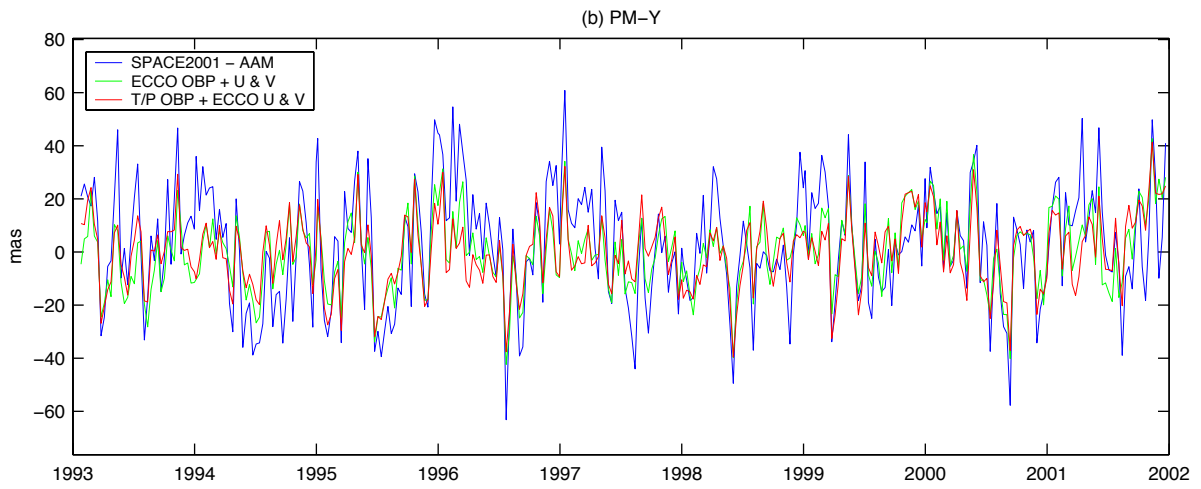
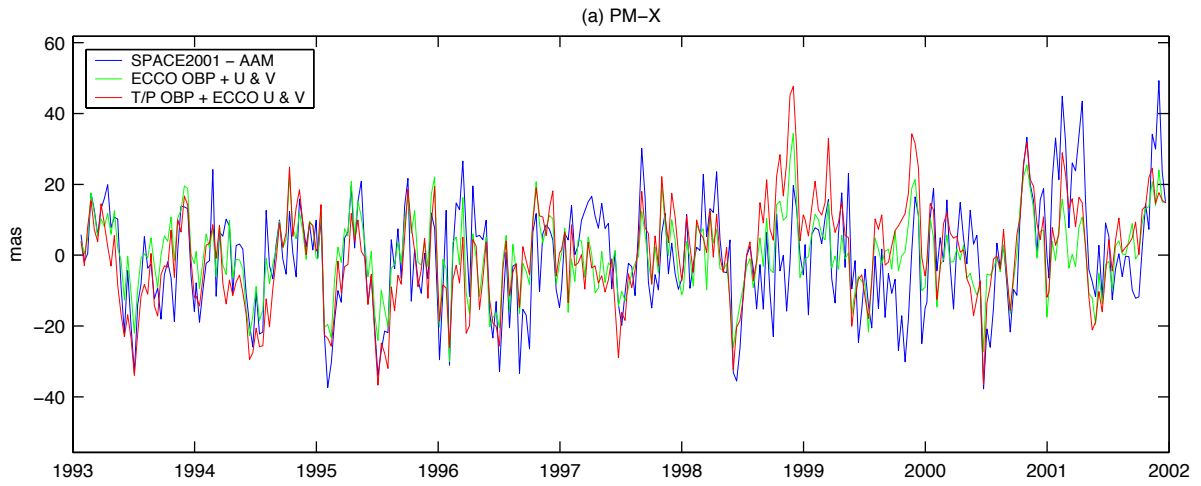


Figure 3

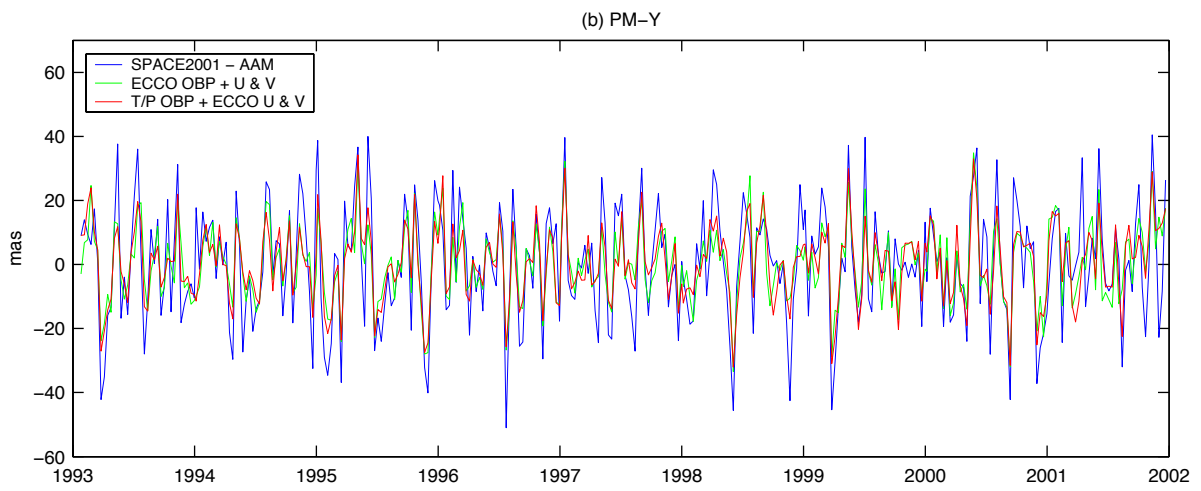
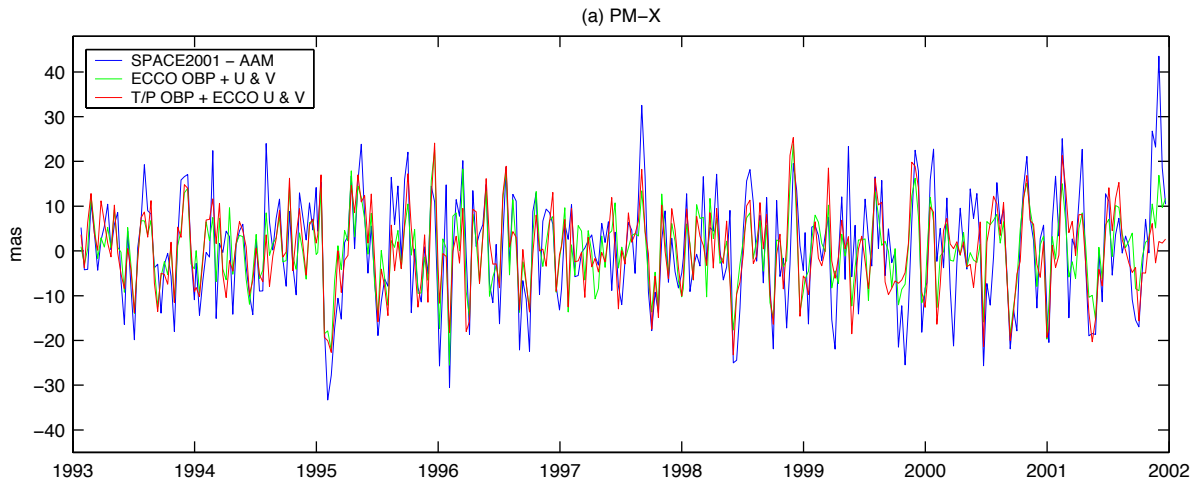


Figure 4

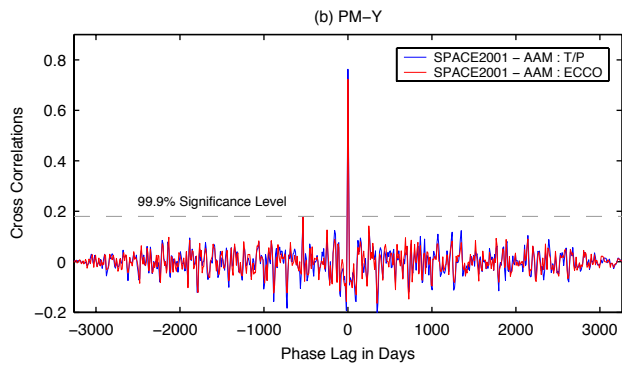
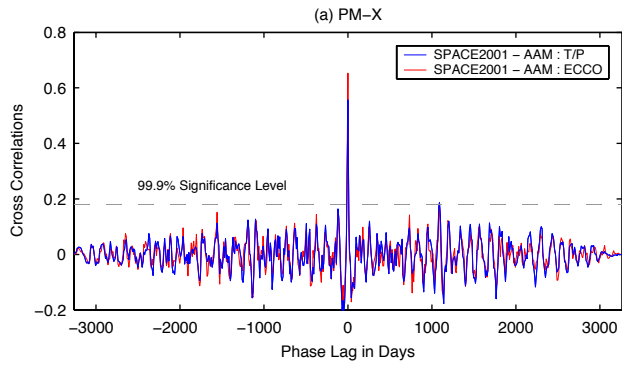


Figure 5

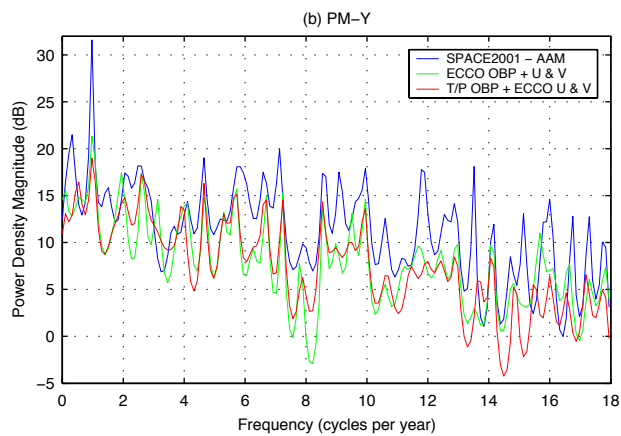
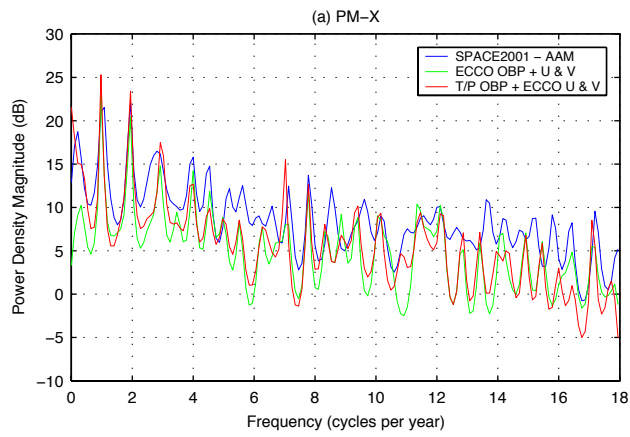


Figure 6

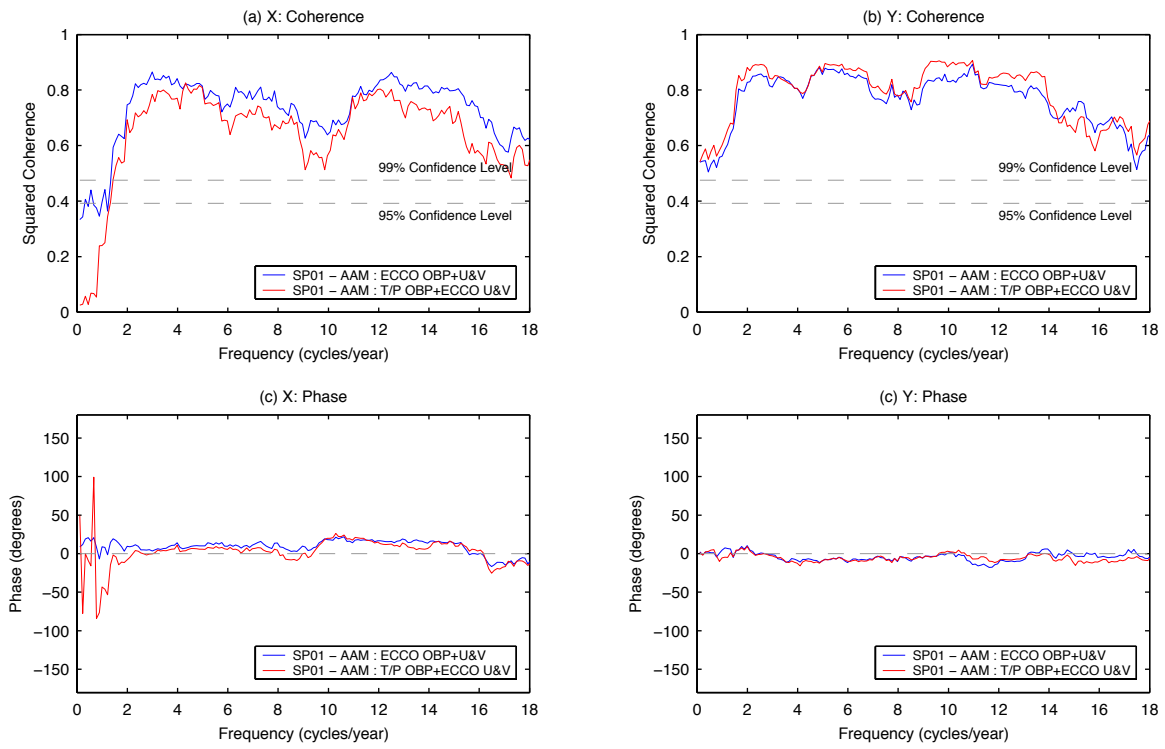


Figure 7

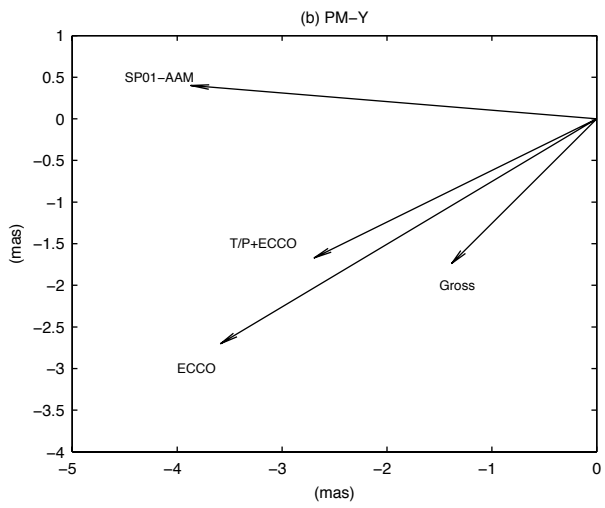
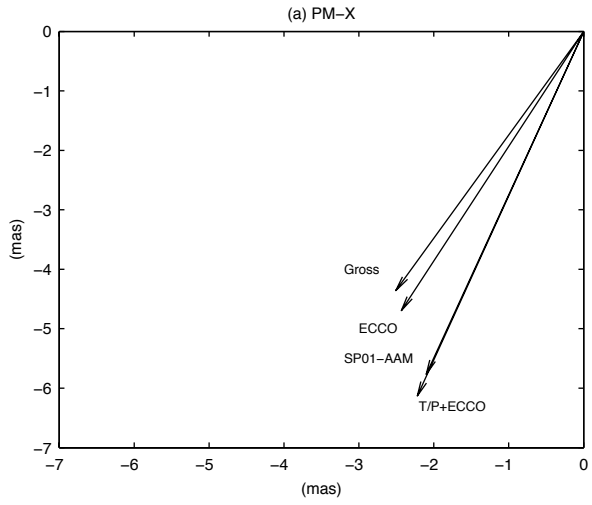


Figure 8